International Journal of Pharmacy and Biological Sciences
ISSN: 2321-3272 (Print), ISSN: 2230-7605 (Online)
IJPBS | Volume 9 | Special Issue 2 | 2019 | 216-225
| Research Article | Biological Sciences |Open Access |MCI Approved|
|UGC Approved Journal|

Thermal and Electrical Transport Properties of O-Substituted Polyanilines Encapsulated with Sio_2 Nanoparticles

S.Jhancy Mary*[1], E.Seetha Rani[2] and R.Suganthi[1]
[1, 2] Department of Chemistry, Auxilium College, Vellore, Tamil Nadu, India.
[1*]Associate Professor of Chemistry, Auxilium College, Vellore, Tamil Nadu, India.

Received: 30 Jan 2019 / Accepted: 25 Feb 2019 / Published online: 01 Apr 2019
Corresponding Author Email: jhancy2011@gmail.com

Abstract
Poly (2-chloroaniline)/SiO_2 and Poly(2-methylaniline)/SiO_2 nanocomposites were synthesized by *in situ* chemical oxidative polymerization technique. The nano composites were characterized by FTIR, NMR and UV- visible spectroscopic techniques, XRD, TEM, TGA and DTA. The thermal stability was confirmed by the IPDT and OI calculations. The electrical conductivity and dielectric properties were investigated. The dielectric constant decreased with increase in frequency in the low frequency region due to electrical relaxation process. At high frequencies, dielectric constant was independent of frequency. At low frequency there was a strong frequency dispersion of permittivity and above 3 Hz, a frequency independent behavior in permittivity was observed.

Keywords
Nanocomposites, Oxidative polymerization, Electrical conductivity, Dielectric, Electrical relaxation.

*****

INTRODUCTION:
Conducting polymer nanocomposites possess the advantages of both low dimensional systems like nanostructure filler and organic conductors like conducting polymer. The reinforcement of polymers is done by fillers, which play a major role in strengthening the properties of the nanocomposites. Uniform dispersion of the nanosized filler particles produces ultra large interfacial area per volume between the filler and the host polymer [1]. Polymer-based composites were reported in the 1960s as a new paradigm in material science. In the past twenty years, three major inorganic materials acting as nanofillers have been used to prepare organic-inorganic nanocomposites: (1) layered materials such as clay[2, 3], (2) tubular materials such as carbon nanotubes (CNTs)[4], and (3) spherical materials such as SiO_2 particles[5] as well as other synthetic materials[6]. Conducting Polymer inorganic nanocomposites attracted both fundamental and practical interest because of their different chemical, biological and physical properties and application in high density magnetic recording, catalysis, magnetic resonance imaging, energy conversion etc. [7-10]. Among all the conducting polymers, Polyaniline is one of the most promising conducting polymers due to its ease of preparation, good environmental stability, better electronic properties, low cost, low density and its applications in electrochromic display, electro

catalysis, rechargeable batteries, sensors and biosensors [11-20].

In the present paper,we report the chemical synthesis, characterization of –Cl and -CH_3 substituted polyaniline- SiO_2 nanocomposites and the thermal and electrical transport properties. An attempt has been taken to understand and compare the influence of SiO_2 on the dielectric properties, impedance and electrical conductivity of poly (2-chloroaniline)-composite-SiO_2 (p2ClAni-SiO_2) and poly (2-methyl aniline)-composite-SiO_2 (p2MeAni- SiO_2) nano composites. The frequency dependence of dielectric constant, dielectric loss, imaginery modulus, real modulus and tan δ are discussed. Complex impedance spectroscopic study was made for understanding the charge transport mechanism [21, 22]. The frequency dependent conductivity and dielectric permittivity provide information on the electronic transport mechanism. It gives an insight into the presence of disorder in the molecular structure of the materials and the process of electrical transport along the polymer chains [22].

MATERIAL AND METHODS:

2-chloroaniline (Avra), 2-methylaniline (LOBA), ammonium per sulphate (SDFCL, 98% pure) and HCl were of analytical grade and used as received. SiO_2 nano particles (particle size of 50 nm) was purchased from Sigma Aldrich. The FT-IR measurements have been carried out using IR Affinity-1 Fourier Transform Infrared Spectrophotometer, Make –Shimadzu in the wave number range 500 cm^{-1} to 4000 cm^{-1}. The UV-Visible analyses were carried out using Perkin Elmer Lambda double beam spectrophotometer in the wavelength range 200-800 nm. XRD analyses were performed on a Bruker AXS D8 Advance using Cu as X-ray source at the wavelength of 1.5406Å of angular range from 3^0 to 135^0. Thermo gravimetric analyses were carried out with a Perkin Elmer STA 6000 from room temperature to 700°C under inert gas atmosphere. Dielectric constants were measured by NOVO CONTROL technologies GmbH and Co. Electrical conductivity measurements were made using German model concept 80 in the frequency range from 10 Hz to 1MHz at room temperature. Z'' Vs Z' complex impedance plots were plotted for the nanocomposites and the bulk resistance (R_b) was evaluated by analyzing the impedance data using zsimpdemo software.

Synthesis of the polymer nanocomposites

The SiO_2 nanocomposites of –Cl and -CH_3 substituted polyanilines have been chemically synthesized by *in situ* chemical oxidative technique by incorporating the nanoparticles obtained from Sigma Aldrich (particle size of 50 nm) during the polymerization. The initiator used was ammonium persulphate and hydrochloric acid was used as the dopant. Sodium lauryl sulphate (SDS) was used as a surfactant but it functionally acted as a dopant as well. The materials were obtained in the form of powder. The composites were obtained in the conducting emeraldine salt forms. After the polymerization was completed the polymer composites were repeatedly washed with deionised water and finally with few drops of acetone to remove the oligomers, dried and stored in air tight vials. The composites were soluble in DMSO, DMF and partially soluble in toluene and chloroform. The percentage yield of the nano composites calculated using the formula, Conversion yield = Polymer yield / Weight of the monomer x 100 are tabulated in Table 1.

Table 1: Percentage Yield of the nanocomposites

Polymer Nanocomposites	% Yield
(p2ClAni-SiO_2)	83.93
(p2MeAni-SiO_2)	93.56

RESULTS:

Infra red spectroscopy

FTIR spectrum of p2ClAni-SiO_2 (Fig 1) gives peaks at 977 cm^{-1} and 827 cm^{-1} characteristics of 1,2,4 tri substituted aromatic rings. A band appearing near 1290 cm^{-1} represents the C-N stretching vibration. The band at approximately 1573 cm^{-1} and 1498 cm^{-1} are due to quinonoid and benzenoid rings respectively. Asymmetric and symmetric aliphatic C-H stretching can be observed at 2924 cm^{-1} and 2852 cm^{-1}. The peak at 748 cm^{-1} is due to -Cl attached to the rings.

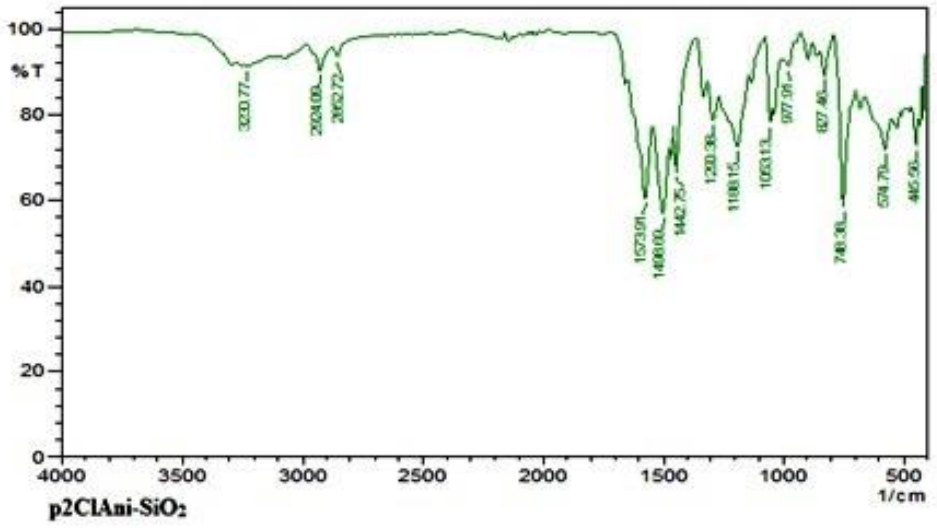

Figure 1: FT- IR spectrum of p2ClAni-SiO_2

The broad absorption peak observed at 3230 cm^{-1} corresponds to the OH groups –present in SiO_2 due to intermolecular hydrogen bonded OH stretching. The bands at about 1188.15 cm^{-1} and 827 cm^{-1} are assigned to the Si-O-Si stretching vibrations and bending vibrations respectively [23].

The IR spectrum gives all the characteristic bands of poly (2-chloroaniline) as well as SiO_2. Hence it was confirmed that the composite formation has taken place. The intensities of all the peaks are reduced due to repeated units in the polymer. The emeraldine salt form of the polymer interacts with SiO_2 nanoparticles through hydrogen bonding type of interaction. The HCl as well as sulphate ions of the sodium lauryl sulphate act as dopants as evidenced from FTIR spectrum.

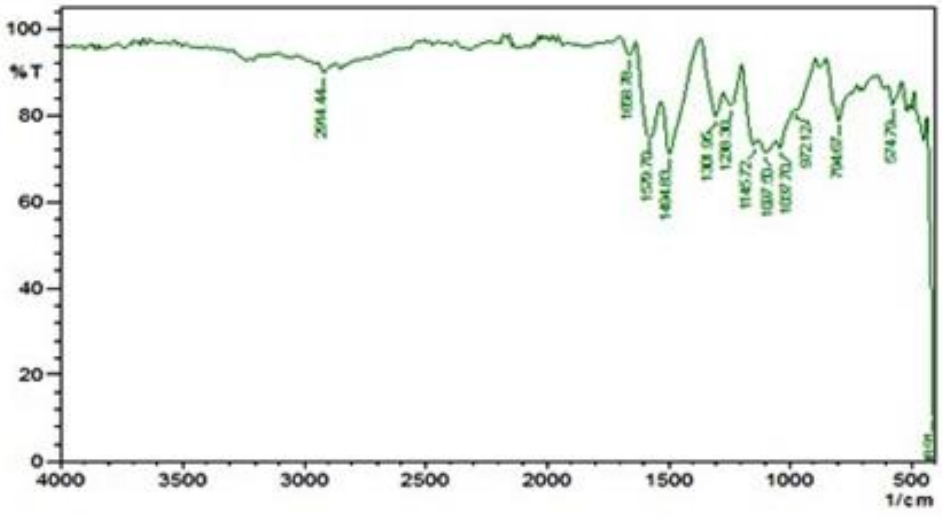

Figure 2: FTIR spectrum of p2MeAni-SiO_2

The Infrared spectrum of p2MeAni-SiO_2 (Fig 2) shows a broad absorption peak around 3200 cm^{-1} and 1301cm^{-1} due to –N-H and C-N stretching of the secondary amine respectively. The peaks at 1579cm^{-1} and 1494 cm^{-1} are assigned to the –C=C- stretching frequencies of quinonoid and benzenoid rings. The peak at 574 cm^{-1} confirms the incorporation of SiO_2 nano particles into the polymer chains. The peak at 1145cm^{-1} is due to the electrical conductivity band. The C-H out of plane bending vibration of the 1, 2, 4 tri substituted benzene rings appear around at 972cm^{-1} and 863cm^{-1}. FTIR spectra indicate peaks of both $–CH_3$ substituted poly aniline and SiO_2.

UV-Visible spectroscopy

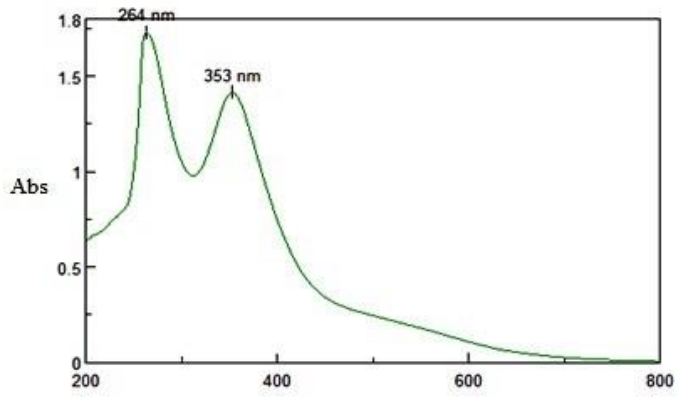

Figure 3: UV-Visible spectrum of p2ClAni-SiO_2

(Fig 3) shows the absorption spectrum of p2ClAni-SiO_2 dissolved in DMSO. The UV absorption band of the polymer composite at 264 nm is due to the π-π* transition. The band at 353 nm is due to n-π*transition. The n-π* transition is due to the transition of lone pair of electrons of the nitrogen atoms to an empty non bonding molecular orbital.

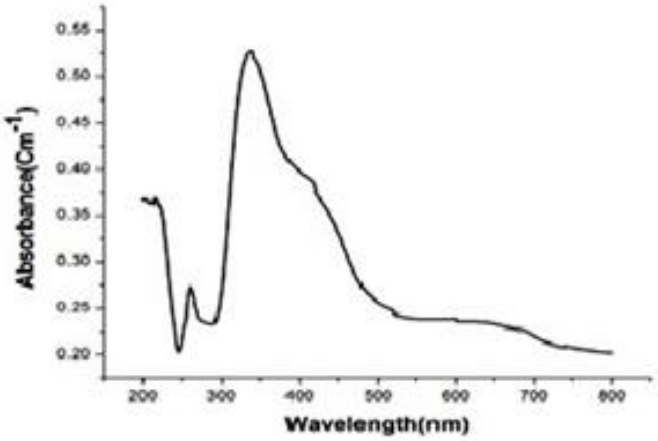

Figure 4: UV-Visible spectrum of p2MeAni-SiO_2

The absorption spectrum (Fig 4) shows major absorptions around 260nm due to π- π^* transition on the polymer chains and the absorption around 350 nm is due to the n- π^* transition of the quinonoid rings and corresponds to the localization of the electron [24]. The polaron band appears around 620 nm.

X-RAY DIFFRACTION STUDIES

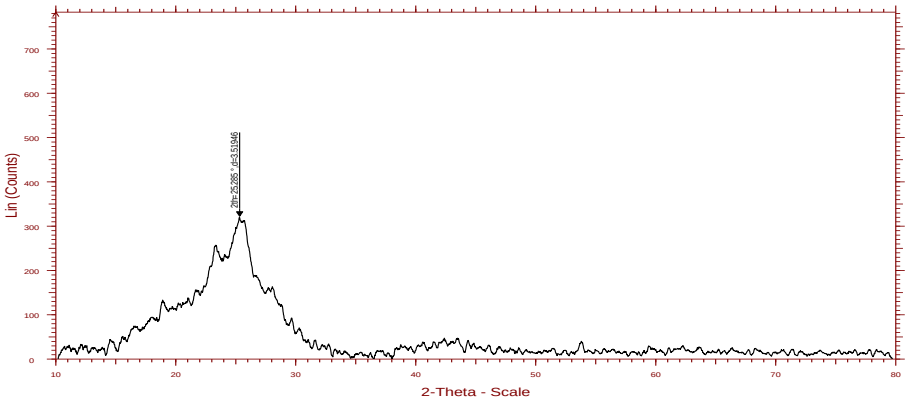

Figure 5: XRD pattern of p2ClAni-SiO_2

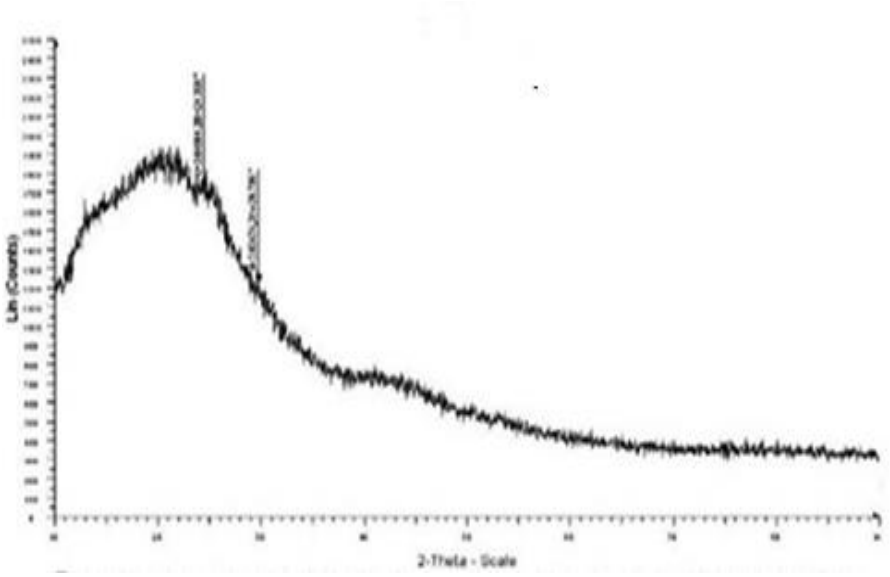

Figure 6: XRD pattern of p2MeAni-SiO_2

The XRD patterns of p2ClAni-SiO_2 and p2MeAni-SiO_2 nanocomposites are shown in Fig 5 and Fig 6. XRD patterns show amorphours nature of the nanocomposites. P2ClAni-SiO_2 composite shows a broad band around 25.285° indicating the amorphous nature of the composite. P2MeAni-SiO_2 composite shows the broad diffraction peaks around at 2θ=24º and 29º due to the amorphous nature.

Thermo gravimetric analysis

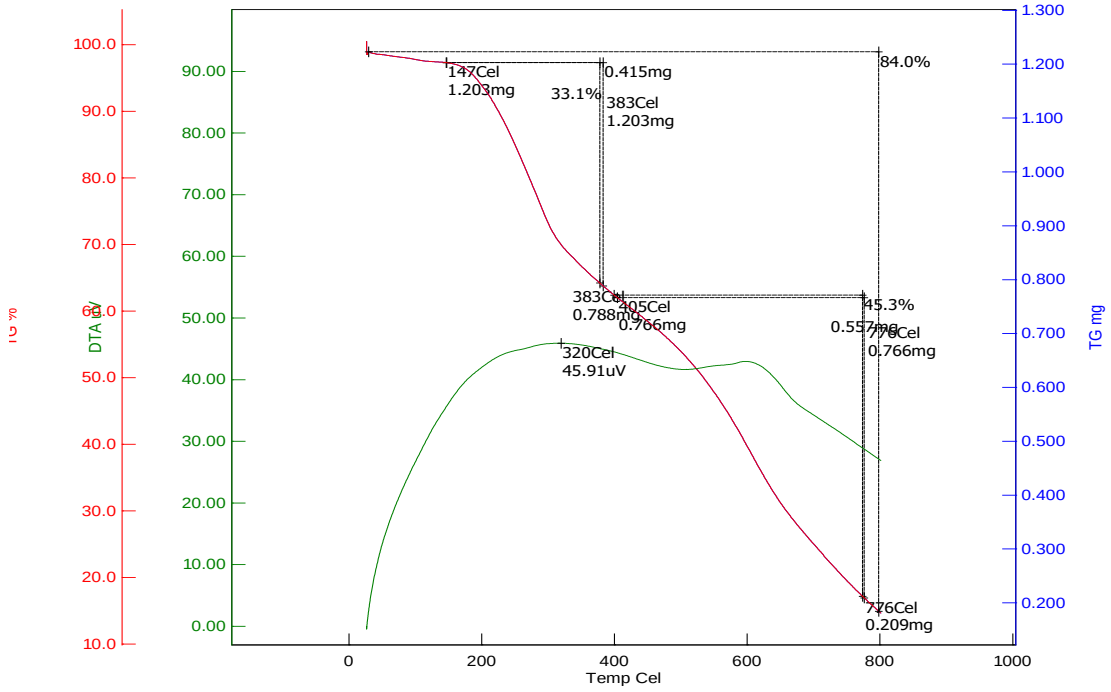

Figure 7: TGA/DTA plots of p2ClAni- SiO_2

The TGA/DTA curves of p2ClAni-SiO_2 are shown in Fig 7. The polymer composite decomposes at 147 °C due to the loss of moisture and volatile impurities. The loss of the dopant takes place at 383 °C and the composite starts decomposing at 777.6°C. The DTA shows the exothermic loss of the dopant and loss of SiO_2 molecules.

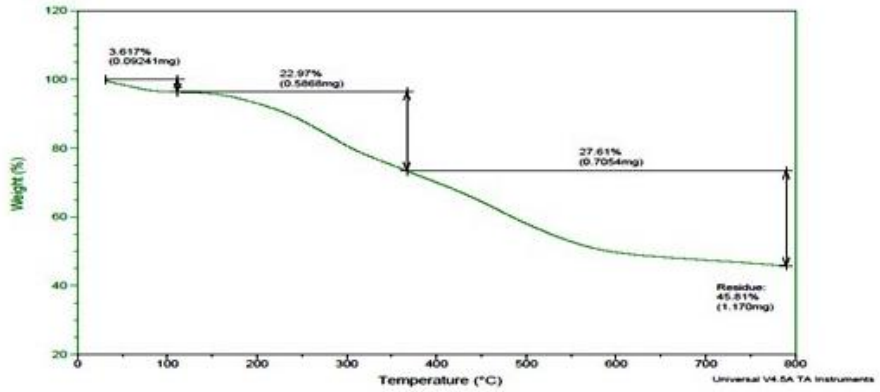

Figure 8: TGA/DTA plots of p2MeAni- SiO_2

The TGA/DTA ofp2MeAni-SiO_2 nano composite shows three step weight loss. At first, the weight loss (3.617%) is due to loss of water and moisture which takes place around 50 -100ºC. The second weight loss up to 350ºC, (22.97 %.) is due to the removal of dopant molecules. In the third step 27.61% decomposition of composite takes place at 350 ºC and ends at 800ºC. The complete decomposition has not taken place. This composite leaves some char content (45.81%). The –Cl substituted polyaniline nano composite is the most stable nanocomposite probably due to the heat resistive property of the chloro atoms.

IPDT is a useful parameter for assessing the overall thermal stability of the polymers during the decomposition process. The area was calculated using the equation,

IPDT (°C) = A × K × (T_f - T_i)

A= (S1+ S2) / (S1+ S2 +S3)

K= (S1+S2)/(S1)

where A is the area ratio of total experimental curve defined by the total TGA thermogram, K is the coefficient, T_i the initial experimental temperature, T_f the final experimental temperature in °C. The oxidation index (OI) was calculated from the weight of the carbon residue, which is related to the flame-retardant capacity of the composites [25] and the values are tabulated in Table 3.

OI × 100 = 17.5 × 0.4 CR

Table 3: IPDT and OI values of the polymer nanocomposites

Polymer nano composites	IPDT	OI
(p2ClAni-SiO_2)	463	0.0146
(p2MeAni-SiO_2)	466	0.0819

Electrical transport properties

Electrical conductivity

The complex impedance plots of solvent free pellets of p2ClAni-SiO_2 and p2MeAni-SiO_2 measured at room temperature in the frequency region 50 Hz to 35 MHz are shown (Fig 9 (i & ii) respectively.

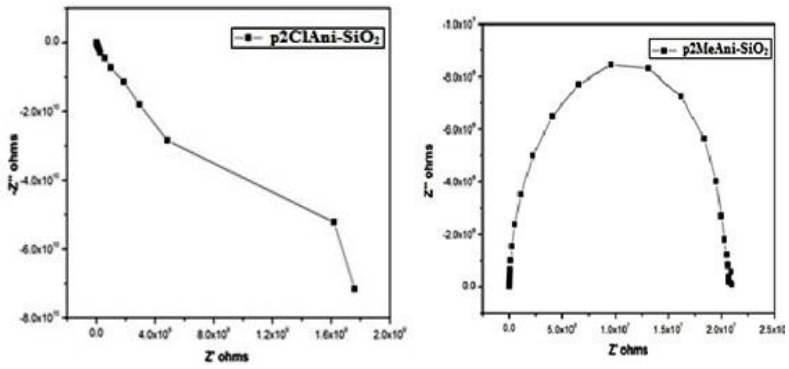

Figure 9 (i) and (ii)

Complex Impedance plots of (i) p2ClAni-SiO_2 (ii) p2MeAni- SiO_2

The total electrical conductivity (σ) values have been calculated using the formula, $\sigma = t / R_b A$ where t is the thickness of the pellet, A is the area covered by the silver electrodes in contact with the material and R_b is the bulk resistance of the material. The zsimpdemo software has been used to get the value of bulk resistance from the intercept on the real axis at the high frequency portion of the Nyquist plots. The electrical conductivity values are tabulated in Table 4.

Table 4: Electrical conductivity values of the nano composites

Nanocomposites	Thickness	R_b	Conductivity
p2ClAni-SiO_2	0.89	$6.43x10^5$	$3.97x10^{-6}$
p2MeAni-SiO_2	0.80	$8.47x10^5$	$2.26x10^{-6}$

Dielectric Properties

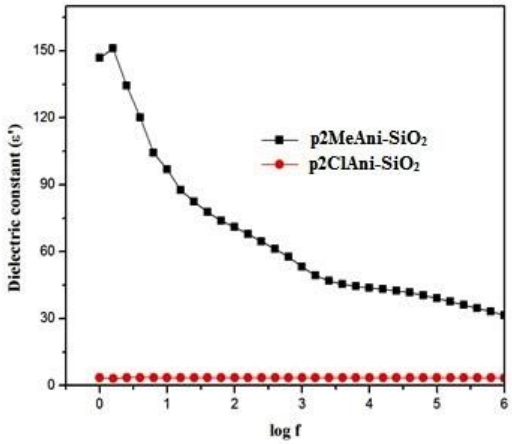

Figure 10: Plots of dielectric constant with frequency

Figure 10 shows the plot of dielectric constant versus frequency. The dielectric constant of p2MeAni-SiO_2 decreases with increase in frequency in the low frequency region due to electrical relaxation process. High dielectric permittivity at low frequency region is due to space charge polarization due to the presence of free charges at the interface [26]. At high frequencies, dielectric constant is independent of frequency as it remains almost constant. At low frequency there is a strong frequency dispersion of permittivity and above 3 Hz there is a frequency independent behavior in permittivity. In the case of p2ClAni-SiO_2, the dielectric constant is independent of frequency.

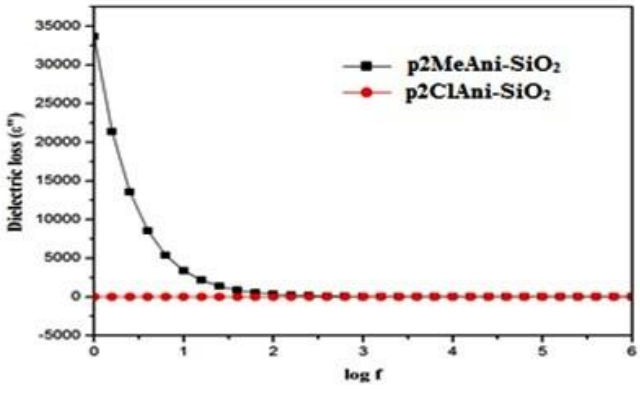

Figure 11: Plots of dielectric loss with frequency

Dielectric loss is a measure of energy dissipated and generally comprises of the contribution from ionic transport as well as polarization of a charge or dipole. In (Fig 11), the dielectric loss is high in $-CH_3$ substituted polyaniline nanocomposites due to free charge motion within the material, a phenomenon leading to conductivity relaxation [27]. Dielectric loss decreases with increases in frequency upto 2 Hz. This is due to the free movement of the charges in the polymer matrix. On increasing the frequency upto 6 Hz there is

no change in dielectric loss as it almost remains constant. In the –Cl substituted polyaniline nano composite, The dielectric loss is independent of frequency.

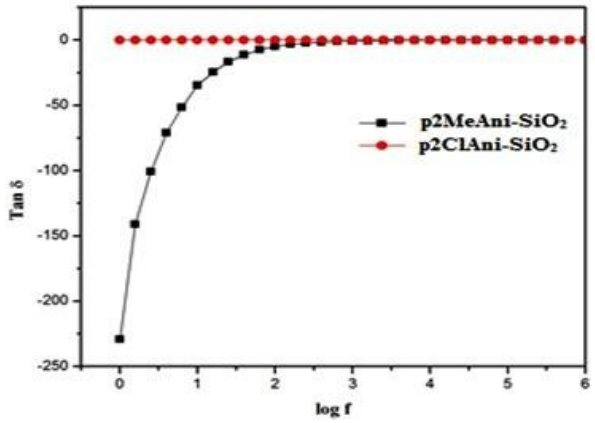

Figure 12: Plots of tan δ with frequency

Figure 12 shows the plot of tan δ with frequency. In p2MeAni-SiO_2 tan δ increases with increase in frequency upto 2 Hz in due to the presence of relaxing dipolar. When frequency greater than 2 Hz is applied tan δ does not vary much with frequency and this is attributed to non-relaxation dipole. A frequency independent behavior is observed in p2ClAni-SiO_2.

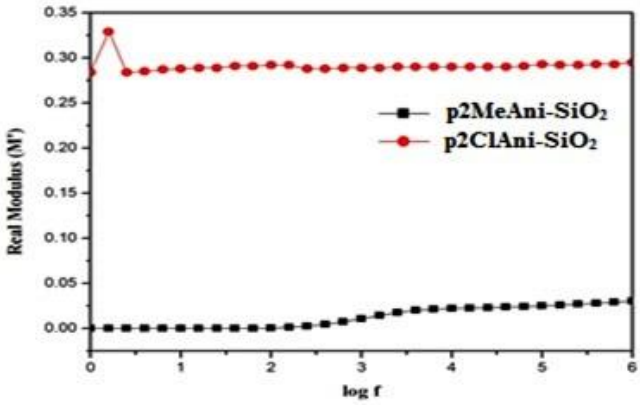

Figure 13: Plots of real modulus with frequency

The normalized modulus spectra in the form of real modulus (M') versus log f is given (Fig 13). The flat portion from low frequency to high frequency in –Cl and -CH_3 substituted polyaniline nano composites is due to large capacitance associated with the electrodes [28].

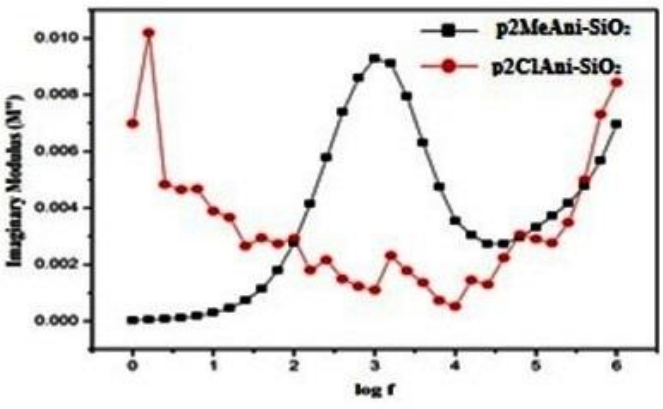

Figure 14: Plots of imaginary modulus with frequency

The imaginary part of M" as a function of frequency for P2ClAni-SiO_2 and P2MeAni-SiO_2 is depicted (Fig14). The spectra exhibit broad peaks at low frequency. The trend is not found to be uniform in p2ClAni-SiO_2 probably due to the electron withdrawing nature of the chloro group.

DISCUSSION:

The FT-IR spectra confirm the existence of benzenoid and quinonoid repeating units with all the corresponding spectral assignments of polymeric backbone. The bands at about 1188.15 $cm^{-1}$and 827 cm^{-1} are assigned to the Si-O-Si stretching vibrations which confirms the incorporation of SiO_2 nanoparticles into the polymeric matrix forming hydrogen bonds. The UV-Visible spectra show the existence of benzenoid rings and quinonoid rings of p2ClAni-SiO_2 and p2MeAni. The XRD patterns of p2ClAni-SiO_2 and p2MeAni-SiO_2 nano composites show amorphous nature of the nanocomposites. The thermal study shows that the polymers and their nanocomposites follow three steps decomposition process. The weight loss corresponds to the loss of moisture, dopant and degradation of polymeric backbone.

The study of electrical conductivity shows that the conductivity values of p2ClAni-SiO_2 and p2MeAni-SiO_2 are $3.97x10^{-6}Scm^{-1}$ and $2.26x10^{-6}$ Scm^{-1} and are semiconducting in nature. The dielectric study shows that the p2MeAni-SiO_2 nanocomposites has capacitance behaviour. It can be used in energy storage and semiconductor devices.

CONCLUSION

In situ chemical oxidative polymerizations were performed in the presence of the host material, SiO_2 to synthesize p2ClAni-SiO_2 and p2MeAni-CuO-SiO_2 nanocomposites. Spectroscopic results confirm the inclusion of SiO_2 nano particles into the-Cl, and $-CH_3$ substituted polyaniline chains. The TGA results confirmed the thermal stability of the nanocomposites. The conductivities as measured by the four-probe technique were of the order of 10^{-6} Scm^{-1} in –Cl and $-CH_3$ substituted nanocomposites. Conductivity values are in the range of semi conductors. These materials will have a significant role to play as energy storage devices.

REFERENCES

[1] Bal S., Samal S., Carbon Nanotube Reinforced Composites – A state of the art. Bull. Mater. Sci, 30(4): 379–386, (2007)

[2] Lee C H., Kato M., Usuki A., Preparation and properties of bio-based polycarbonate/clay nanocomposites. J. Mater. Chem, 21(19): 6844-6847, (2011)

[3] Chang K. C., Hsu C. H., et al., Advanced anticorrosive coatings prepared from electroactive polyimide/graphene nanocomposites with synergistic effects of redox catalytic capability and gas barrier properties. Express Polym. Lett, 8(4): 243- 255(2014)

[4] Minus M.L., Chae H. G., Kumar S., Polyethylene crystallization nucleated by carbon nanotubes under shear. ACS Appl. Mater. Interfaces, 4 (1): 326-330, (2014)

[5] Hu X L., Hou G-M., Zhang M Q., Rong M Z., Ruan W H., and Giannelis E P., A new nanocomposite electrolyte based on poly (vinyl alcohol) incorporating hyper grafted nano-silica. J. Mater. Chem, 22: 18961-18967, (2012)

[6] Tang CW., Li B., Sun L., Lively B., Zhong WH., The effects of nanofillers, stretching and recrystallization on microstructure, phase transformation and dielectric properties in PVDF nanocomposites. Eur. Polym. J, 48(6): 1062- 1072, (2012)

[7] Tartaj P., Morales MD., Veintemillas- Verdaguer S., Gonzalez-CarrenoT and Serna C.J., The preparation of magnetic nanoparticles for applications in biomedicine. J. Phys. D, 36(13): 182–197, (2003).

[8] Sun C., Lee JSH and Zhang M., Magnetic nanoparticles in MR imaging and drug delivery.Adv Drug Deliv, 60(11): 1252-1265, (2008)

[9] Li P., Miser DE., Rabiei S., Yadav RT., Hajaligol MR., The removal of carbon monoxide by iron oxide nanoparticles. Appl. Catal B, 43: 151–162, (2003)

[10] Sun S., Murray CB., Weller D., Folks L and Moser A.,Monodisperse FePt nanoparticles and ferromagnetic FePt nanocrystal superlattices. Science, 287(5460): 1989–1992, (2000)

[11] Chandrakanthi R. L. N., Careem M. A., Preparation and characterization of CdS and Cu_2Snanoparticle/polyaniline composite films. Thin Solid Films: 417: 51-56, (2002)

[12] Somani P. R., Marimuthu R et al., Studies on Electrical and Sensing Properties of Polyaniline / Iron Oxide (Γ-Fe2O3) Nanocomposites. Synth.Met, 45-52, (1999)

[13] He Y. J., Synthesis of polyaniline/nano-CeO_2 composite microspheres via a solid-stabilized emulsion route. Mater. Chem. Phys, 92: 134–137, (2005)

[14] Geng L., Zhao Y., Huang X., Wang S., Zhang S., and Wu, Properties and Application of polymer/Clay and Carbon-Based Polymer Nanocomposites. J. Nature publisher B, 20: 568–572 (2007)

[15] Yu S., Xi M., Jin X., Han K., Wang Z., and Zhu H., Preparation and photoelectron catalytic properties of polyaniline-intercalated layered manganese oxide film. Catal. Commun, 11(14): 1125–1128, (2010)

[16] Buron C. C., Lakard B., FMonnin A.V., Moutarlier., and Lakard S., Synth Met., 2162-2169, (2011)

[17] Adhikari B., Majumdar S., Polymer in Sensor Application, Prog. Polym.Sci, 679, (2004)

[18] McQuade D. T., Pullen A. E., Swager T. M., Conjugated polymer based chemical sensor. Chem. Rev. 100: 7, 2537-2574, (2000)

[19] Gerard M., Chaubey A., Malhotra B. D., application of conducting polymers to biosensors. Biosens. Bioelectron, 17 (5): 345, (2002)

[20] Chiang J. P., MacDiarmid A. G., Polyaniline: Protonic acid doping of the emeraldine form to the metallic regime. Synth. Met, 13(1): 193, (1986)

[21] Mc Call R.P., Scherr E.M., Mac Diarmid A.G. and Epstein A. Anisotropic optical properties of an oriented-emeraldine-base polymer and an emeraldine-hydrochloride-salt polymer. Phys. Rev. B, 50(8): 5094. (1994)

[22] Epstein A.J., and Mac Diarmid A.G., Secondary Doping" - A New Concept in Conducting Polymers. Macromol. Symp, 51: 11, (1991)

[23] Liu B.T., Tang S.J., Yu Y.Y., and Lin S.H., High-refractive-index polymer/inorganic hybrid films containing high TiO_2 contents. Colloids Surf, 377(1): 138-143, (2011)

[24] Mattoso L.H.C., Manohar S.K., MacDiarmid A.G., Epstein A., Studies on the chemical syntheses and on the characteristics of polyaniline derivatives. J. Polym.Sci. Part A, Polym. Chem, 33(8): 1227, (1995)

[25] Kumar H., Anilkumar A. and Siddaramaiah, Thermal degradation kinetics of nylon6/GF/crysnano nanoclay nanocomposites by TGA. Chem.Ind.Chem. Eng.Q, 17(2): 141–151, (2011)

[26] Kim H.M., Lee C.Y. and Joo J., AC Dielectric Relaxation of Lightly Hydrochloric-Acid (HCl)-doped Polyanilines J. Korean. Phys. Soc, 36(6): 371-375, (2000)

[27] J.Malathi et al., Structural, thermal and electrical properties of PVA-$LiCF_3SO_3$ polymer electrolyte. J. Non-Cryst. Solids, 356(43): 2277-2281, (2010)

[28] Hodge I.M., Ingram M.D., West A.R., Impedance and modulus spectroscopy of polycrystalline solid electrolyte. J. Electro. Anal. Chem, 74(2): 125-143, (1976)